Structural Engineering and Mechanics, *Vol. 47, No. 1 (2013) 27-44*
DOI: http://dx.doi.org/10.12989/sem.2013.47.1.027

Analysis of thermo-rheologically complex structures with geometrical nonlinearity

Fatin F. Mahmoud[a], Ahmed G. El-Shafei[b] and Mohamed A. Attia[*]

Department of Mechanical Design and Production Engineering, College of Engineering, Zagazig Univeristy, Zagazig, 44511, Egypt

(Received May 12, 2012, Revised May 7, 2013, Accepted July 3, 2013)

Abstract. A finite element computational procedure for the accurate analysis of quasistatic thermo-rheological complex structures response is developed. The geometrical nonlinearity, arising from large displacements and rotations (but small strains), is accounted for by the total Lagrangian description of motion. The Schapery's nonlinear single-integral viscoelastic constitutive model is modified for a time-stress-temperature-dependent behavior. The nonlinear thermo-viscoelastic constitutive equations are incrementalized leading to a recursive relationship and thereby the resulting finite element equations necessitate data storage from the previous time step only, and not the entire deformation history. The Newton-Raphson iterative scheme is employed to obtain a converged solution for the non-linear finite element equations. The developed numerical model is verified with the previously published works and a good agreement with them is found. The applicability of the developed model is demonstrated by analyzing two examples with different thermal/mechanical loading histories.

Keywords: thermo-rheological complex material (TCM); nonlinear Schapery's model; geometrical nonlinearity; finite element method (FEM)

1. Introduction

Many engineering materials that cannot be adequately modeled using the classical elasticity formulation; one category of such materials is the set of viscoelastic materials. The theoretical foundations for viscoelasticity are well established by Ferry (1980) and Christensen (1982). Many viscoelastic materials exhibit linear or nonlinear behavior under combined structural and environmental loadings. The nonlinear viscoelastic response, which often occurs at high load level and elevated temperatures, is indicated by non-constant material properties.

Viscoelastic materials can be categorized as thermo-rheological simple materials (TSM) or thermo-rheological complex materials (TCM). In TSM, the temperature effect is incorporated only through a time-scale shift factor, Ferry (1980). Idealizing thermo-viscoelastic responses of materials as TSM is sufficient when the materials are subjected to moderate temperature changes and temperature does not vary with time or when the materials are under constant temperature

∗Corresponding author, Assistant Professor, E-mail: omarmadly@yahoo.com
[a]Professor
[b]Associate Professor

http://www.techno-press.org/?journal=sem&subpage=8 ISSN: 1225-4568 (Print), 1598-6217 (Online)

rates and constant mechanical loads. Other materials that do not belong to the TSM are referred to TCM, in such materials; temperature influences the material's initial, instantaneous elastic, and time-dependent, transient, properties. Further discussions regarding both TSM and TCM can be found in Peretz and Weitsman (1983), Harper and Weitsman (1985).

Numerical methods provide a powerful framework for obtaining approximate solutions to linear viscoelasticity problems. In particular, the FEM has been employed successfully in the analysis of viscoelastic bodies by many researchers. Taylor *et al.* (1970) used the FEM in conjunction with a recurrence relation to solve viscoelasticity problems such that data from only the previous time step (as opposed to the entire deformation history) is needed in determining a body's configuration at the current time step. A similar recursive approach was used by Feng (1992) for viscoelastic materials described by the Voltera integral equation. Additional general FE formulations for viscoelastic continua can be found in (Areias and Matous 2008, Guedes 2010, Mahmoud *et al*. 2011). The recursive method has also been used for solving nonlinear viscoelastic constitutive equations.

The Schapery's nonlinear viscoelastic model, Schapery (1969) has been extensively applied for isotropic and anisotropic materials. Lai and Bakker (1996) developed a recursive algorithm including nonlinear effects due to temperature and physical aging in terms of the reduced time functions. Haj-Ali and Muliana (2004) formulated a recursive scheme of the Schapery's stress-dependent viscoelastic constitutive models for isotropic materials based on decoupling the deviatoric and volumetric parts. Muliana (2008) extended this scheme of the Schapery theory and implemented it in Abaqus FE package to represent the TCM behavior at small deformations.

Considering geometrical nonlinearity in viscoelasticity, Rogers and Lee (1962) developed a direct FE model for solving the nonlinear integro-differential equations that arise in the finite deflection of a thin linear viscoelastic beam due to constant load history. Roy and Reddy (1988) analyzed the geometrically nonlinear deformations of adhesive joints using an updated Lagrangian FE formulation. The adhesive was modeled as nonlinear viscoelastic using a constitutive law proposed by Schapery (1969). Touati and Cederbaum (1998a) used Schapery's nonlinear viscoelastic theory to study the postbuckling response of laminated plates with initial imperfections. Payette and Reddy (2010) presented a FE model using a recursive relation for solving quasi-static viscoelastic Euler-Bernoulli and Timoshenko beams with linear mechanical properties. Large transverse displacements, moderate rotations and small strains were allowed Further studies on the numerical modeling of linear/nonlinear viscoelasticity problems with large mechanical deformations can be found in Lin (2001), Bonet (2001), and Vaz and Caire (2011).

For the FE modeling of thermo-viscoelastic problems including geometrical nonlinearities, Holzapfel and Reiter (1995), Reese and Wriggers (1998), Johnson and Chen (2005) presented time-integration procedures for coupled thermo-viscoelastic behaviors for small and large deformation problems. Constitutive equations were derived from the Maxwell mechanical analog model with constant material properties. Reese and Govindjee (1997) extended a model for finite deformation viscoelasticity that utilizes a nonlinear evolution law to include thermal effects. Khan *et al*. (2006) developed a phenomenological one-dimensional constitutive model, characterizing the complex nonlinear finite thermo-mechanical behavior of viscoelastic polymers. Their simple differential form model is based on a combination of linear and nonlinear springs with dashpots. Khan *et al*. (2010) studied the characterization of the large deformation response of two elastomers over a wide range of strain rates and temperatures.

As noted, majority of the cited references deals with the FE modeling of small/large deformations structures based on the assumptions that the material behaves linear thermo-

viscoelasticity. The original contribution of this work is to develop and implement a FE model capable of analyzing quasistatic nonlinear viscoelastic structures. The developed model accounts for TCM behavior and geometrical nonlinearity arising from large displacements and rotations (but small strains) under different thermo-mechanical loading histories. The Schapery's nonlinear viscoelastic model is adopted and modified with an integral form to include time-stress-temperature dependent behavior. The constitutive equations are transformed into an incremental form suitable for the FE formulations. This results in a recursive relationship, which allows bypassing the need to store entire strain histories, only the previous time step is needed. The geometrical and material nonlinearities are modeled in the framework of the total Lagrangian formulation. The Newton-Raphson iterative scheme is utilized to obtain the converged solution at the end of each time increment. The developed procedure is implemented into 2D time dependent nonlinear FE model. Obtained results are compared with benchmark results. Numerical results for different thermo-mechanical loading conditions are presented to show the significance of material nonlinearity and thermo-rheological behavior on the system response.

2. The nonlinear thermo-viscoelastic constitutive model

The Schapery uniaxial stress-strain history relationship, Schapery (1969, 1997), is modified for a time-stress-temperature-dependent behavior, which refers to a class of TCM, of non-aging materials. For large displacements and rotations with small strain assumption, the uniaxial relationship relating the second Piola Kirchhoff stress ${}^{t}S$ and the Green-Lagrange strain ${}^{t}e$ can be expressed as

$$ {}^{t}e \equiv e(t) = g_0({}^{t}S, {}^{t}\theta) D_0 \, {}^{t}S + g_1({}^{t}S, {}^{t}\theta) \int_0^t \Delta D^{({}^{t}\Psi - {}^{\tau}\Psi)} \frac{d}{d\tau} \left[g_2({}^{\tau}S, {}^{\tau}\theta) {}^{\tau}S \right] d\tau + \int_0^t \alpha({}^{\tau}\theta) \frac{d({}^{\tau}\theta)}{d\tau} d\tau \quad (1) $$

where ${}^{t}\theta$ is the current applied temperature, D_0 is the instantaneous elastic compliance, $\Delta D(\psi)$ is the transient creep compliance. ψ is the reduced time, which is given by

$$ {}^{t}\Psi \equiv \Psi(t) = \int_0^t \frac{dt}{a_\sigma \, a_\theta} \quad \text{and} \quad {}^{\tau}\Psi \equiv \Psi(\tau) = \int_0^\tau \frac{d\tau}{a_\sigma \, a_\theta} \quad (2) $$

g_0, g_1, and g_2 are the nonlinear parameters related to stress or strain status. The parameter g_0 is related to the nonlinear instantaneous compliance, g_1 is associated with the nonlinear transient compliance, and g_2 is related to the loading rate effect on nonlinear response. a_θ is the temperature shift factor and a_σ is the strain or stress shift factor. The transient compliance $\Delta D(\psi)$ can be represented using the Prony series,

$$ \Delta D({}^{t}\Psi) = \sum_{n=1}^{N} D_n \left[1 - \exp(-\lambda_n \, {}^{t}\Psi) \right] \quad (3) $$

where D_n is the *nth* coefficient of the Prony series and λ_n is the *nth* retardation time. Both D_n and λ_n are assumed to be time-stress-temperature independent. Generally, the coefficient of thermal expansion α is assumed to be temperature-dependent. For constant α, the thermal strain appears in Eq. (1), ${}^{t}e_{th}$ is reduced to

$$ {}^{t}e_{th} = \int_{0}^{t} \alpha({}^{\tau}\theta) \frac{d({}^{\tau}\theta)}{d\tau} d\tau = \alpha \Delta^{\tau}\theta = \alpha \left({}^{t}\theta - \theta_{ref} \right) \tag{4} $$

where θ_{ref} is the reference temperature.

The convolution form expressed by Eq. (1) can be generalized for multiaxial constitutive relations for isotropic TCM. This can be done by decoupling the deviatoric and volumetric strain-stress relations and thermal strains as

$$ {}^{t}e_{ij} = {}^{t}e_{ij}^{d} + \frac{1}{3} {}^{t}e_{kk}\, \delta_{ij} + {}^{t}e_{th}\, \delta_{ij} \tag{5} $$

Applying the Schapery integral constitutive model, the deviatoric and volumetric mechanical strains can be expressed as

$$ {}^{t}e_{ij}^{d} = \frac{1}{2} \left[{}^{t}g_0 J_0 \, {}^{t}S_{ij}^{d} + {}^{t}g_1 \int_{0}^{t} \Delta J^{({}^{t}\Psi - {}^{\tau}\Psi)} \frac{d}{d\tau} \left({}^{t}g_2 S_{ij}^{d} \right) d\tau \right] \tag{6} $$

$$ {}^{t}e_{kk} = \frac{1}{3} \left[{}^{t}g_0 B_0 \, {}^{t}S_{kk} + {}^{t}g_1 \int_{0}^{t} \Delta B^{({}^{t}\Psi - {}^{\tau}\Psi)} \frac{d}{d\tau} \left({}^{t}g_2 \, {}^{\tau}S_{kk} \right) d\tau \right] \tag{7} $$

where e_{ij} is the deviatoric strain and e_{kk} is the volumetric strain. J_0 and B_0 are instantaneous elastic shear compliance and instantaneous elastic bulk compliance, respectively. ΔJ and ΔB are transient shear compliance and transient bulk compliance, respectively. To simplify material characterization, the Poisson's ratio v is assumed to be time independent. This leads to the following expressions of the compliances

$$ \begin{aligned} J_0 &= 2(1+\nu) D_0, \qquad \Delta J(\Psi) = 2(1+\nu) \Delta D(\Psi), \\ B_0 &= 3(1-2\nu) D_0, \text{and} \quad \Delta B(\Psi) = 3(1-2\nu) \Delta D(\Psi) \end{aligned} \tag{8} $$

3. The mathematical model

The problem to be solved in this study is the quasistatic isotropic thermo-viscoelastic initial-boundary value problem exhibiting both material and geometrical nonlinearities with TCM behavior. Consider a general 2D domain Ω, bounded by surface Γ, and subjected to thermal/mechanical loading. A concise statement of this problem, formulated in the context of continuum mechanics, can be formally stated as follows.

The equilibrium equations: for a quasi-static assumption, the applied loads vary slowly with time, and thus the inertial term may be neglected in the equations of motion. For such a condition with large deformations, the equilibrium equations can be described as; Fung and Tong (2001)

$$ \frac{\partial}{\partial x_{0j}} \left(S_{ji} \frac{\partial x_i}{\partial x_{0i}} \right) + \rho f_i = 0 \qquad \text{in } (\Omega, t) \tag{9} $$

where S_{ji} is the 2nd Piola Kirchhoff stress tensor, ρ is the body density and f_i is the body force.

The kinematic constraints: large deformations are expressed by the Green strain-displacement relation

$$e_{ij} = 0.5\left(u_{i,j} + u_{j,i} + u_{k,i}u_{k,j}\right) \tag{10}$$

The boundary conditions

$$u_i = \bar{u}_i \quad (\text{on}\,\Gamma_d) \qquad \text{and} \qquad S_{ij}n_j = F_i \quad (\text{on}\,\Gamma_f) \tag{11}$$

where $\bar{u}_i$ is the prescribed displacement on the boundary Γ_d, n_j is the unit outer normal vector at the point of interest and F_i is the prescribed surface traction on the boundary Γ_f.
The initial conditions

$${}^{t}u_i = u_i', \quad {}^{t}\theta = \theta', \text{and} \quad {}^{t}S_{ij} = S_{ij}' \quad (in\ \Omega, t = 0) \tag{12}$$

where u_i', θ', and S_{ij}' are the initial values of displacement, temperature, and 2nd Piola Kirchhoff stresses respectively.

4. The incremental form of the Schapery nonlinear constitutive model

An incremental form of the Schapery nonlinear constitutive model will be derived leading to a recursive relationship, which will be more amenable to FE implementation. The resulting FE equations necessitate data storage from the previous time step only, and not the entire deformation history. By substitution of Eqs. (3) and (8) into Eqs. (6)-(7) and assuming that the term ${}^{\tau}g_2{}^{\tau}S$ to be linear over the current time increment, the deviatoric and volumetric strains can be written in terms of hereditary integral formulation and as follows

$$\begin{aligned} {}^{t}e_{ij}^{d} &= \frac{1}{2}\left(g_0 J_0\, {}^{t}S_{ij}^{d} + {}^{t}g_1\, {}^{t}g_2\, {}^{t}S_{ij}^{d} \sum_{n=1}^{N} J_n - {}^{t}g_1 \sum_{n=1}^{N} J_n\, {}^{t}q_{ij,n} \right) \\ \text{where } {}^{t}q_{ij,n} &= \int_0^t \exp\left[-\lambda_n \left({}^{t}\Psi - {}^{\tau}\Psi\right)\right] \frac{d\left[{}^{\tau}g_2\, {}^{\tau}S_{ij}^{d}\right]}{d\tau} d\tau \end{aligned} \tag{13}$$

$$\begin{aligned} {}^{t}e_{kk} &= \frac{1}{3}\left({}^{t}g_0 B_0\, {}^{t}S_{kk} + {}^{t}g_1\, {}^{t}g_2\, {}^{t}S_{kk} \sum_{n=1}^{N} B_n - {}^{t}g_1 \sum_{n=1}^{N} B_n\, {}^{t}q_{kk,n} \right) \\ \text{where } {}^{t}q_{kk,n} &= \int_0^t \exp\left[-\lambda_n \left({}^{t}\Psi - {}^{\tau}\Psi\right)\right] \frac{d\left[{}^{\tau}g_2\, {}^{\tau}S_{kk}\right]}{d\tau} d\tau \end{aligned} \tag{14}$$

Applying the recursive integration method to Eqs. (13)-(14) by splitting the integration into two parts, consequently

$${}^{t}q_{ij,n} = \exp\left[-\lambda_n \Delta {}^{t}\Psi\right]^{t-\Delta t} q_{ij,n} + \left(\frac{1 - \exp\left[-\lambda_n \Delta {}^{t}\Psi\right]}{\lambda_n \Delta {}^{t}\Psi} \right) \left[{}^{t}g_2\, {}^{t}S_{ij}^{d} - {}^{t-\Delta t}g_2\, {}^{t-\Delta t}S_{ij}^{d} \right] \tag{15}$$

$${}^{t}q_{kk,n} = \exp\left[-\lambda_n \Delta {}^{t}\Psi\right]^{t-\Delta t} q_{kk,n} + \left(\frac{1 - \exp\left[-\lambda_n \Delta {}^{t}\Psi\right]}{\lambda_n \Delta {}^{t}\Psi} \right) \left[{}^{t}g_2\, {}^{t}S_{kk} - {}^{t-\Delta t}g_2\, {}^{t-\Delta t}S_{kk} \right] \tag{16}$$

The variables ${}^{t-\Delta t}q_{ij,n}$ and ${}^{t-\Delta t}q_{kk,n}$ are the shear and volumetric hereditary integrals at the end of the previous time t-Δt for every term in the Prony exponential series, respectively. These variables are considered as the history state variable that needed to be stored at the end of each time increment. Substituting Eqs. (15)-(16) into Eqs. (6)-(7) yields the following incremental form for deviatoric and volumetric mechanical strains

$$\Delta {}^{t}e_{ij}^{d} = {}^{t}\overline{\mathrm{J}}\,{}^{t}S_{ij}^{d} - {}^{t-\Delta t}\overline{\mathrm{J}}^{t-\Delta t}S_{ij}^{d} - \frac{1}{2}\sum_{n=1}^{N} J_n \left({}^{t}g_1 \exp\left[-\lambda_n \Delta {}^{t}\Psi\right] - {}^{t-\Delta t}g_1 \right) {}^{t-\Delta t}q_{ij,n} + \frac{1}{2}\,{}^{t-\Delta t}g_2\,{}^{t-\Delta t}S_{ij}^{d} \sum_{n=1}^{N} J_n \left({}^{t}g_1 \frac{1-\exp\left(-\lambda_n \Delta {}^{t}\Psi\right)}{\lambda_n \Delta {}^{t}\Psi} - {}^{t-\Delta t}g_1 \frac{1-\exp\left(-\lambda_n \Delta {}^{t-\Delta t}\Psi\right)}{\lambda_n \Delta {}^{t-\Delta t}\Psi} \right) \tag{17}$$

$$\Delta {}^{t}e_{kk} = {}^{t}\overline{\mathrm{B}}\,{}^{t}S_{kk} - {}^{t-\Delta t}\overline{\mathrm{B}}^{t-\Delta t}S_{kk} - \frac{1}{3}\sum_{n=1}^{N} B_n \left({}^{t}g_1 \exp\left[-\lambda_n \Delta {}^{t}\Psi\right] - {}^{t-\Delta t}g_1 \right) {}^{t-\Delta t}q_{kk,n} + \frac{1}{3}\,{}^{t-\Delta t}g_2\,{}^{t-\Delta t}S_{kk} \sum_{n=1}^{N} B_n \left({}^{t}g_1 \frac{1-\exp\left(-\lambda_n \Delta {}^{t}\Psi\right)}{\lambda_n \Delta {}^{t}\Psi} - {}^{t-\Delta t}g_1 \frac{1-\exp\left(-\lambda_n \Delta {}^{t-\Delta t}\Psi\right)}{\lambda_n \Delta {}^{t-\Delta t}\Psi} \right) \tag{18}$$

where

$${}^{t}\overline{\mathrm{J}} = \frac{1}{2}\left({}^{t}g_0 J_0 + {}^{t}g_1\,{}^{t}g_2 \sum_{n=1}^{N} J_n \left[1 - \frac{1-\exp\left(-\lambda_n \Delta {}^{t}\Psi\right)}{\lambda_n \Delta {}^{t}\Psi} \right] \right) \tag{19}$$

$${}^{t}\overline{\mathrm{B}} = \frac{1}{3}\left({}^{t}g_0 B_0 + {}^{t}g_1\,{}^{t}g_2 \sum_{n=1}^{N} B_n \left[1 - \frac{1-\exp\left(-\lambda_n \Delta {}^{t}\Psi\right)}{\lambda_n \Delta {}^{t}\Psi} \right] \right) \tag{20}$$

The above equations are used to determine the unknown stresses increments for a given strains increments and the previous history rate, i.e. hereditary integrals. The main difficulty is that the nonlinear stress functions at the current time are not known. Therefore, an iterative procedure is needed for the stress correction. An expressions for the approximate or trial incremental stresses can be obtained from Eqs. (17)-(18) by assuming

$${}^{t}a = {}^{t-\Delta t}a, \quad \Delta {}^{t}\Psi = \Delta {}^{t-\Delta t}\Psi, \text{and} \quad {}^{t}g_j = {}^{t-\Delta t}g_j, \quad j = 0,1,2 \tag{21}$$

This leads to the following approximate incremental form for 2nd Piola Kirchhoff stresses

$$\Delta {}^{t}S_{ij} = \frac{1}{\left({}^{t}g_0 D_0 + {}^{t}g_1\,{}^{t}g_2\,{}^{t}\overline{\mathrm{H}} \right)} \left(\begin{array}{l} \dfrac{1}{(1+\nu)}\left[\Delta {}^{t}e_{ij} - \delta_{ij}\Delta {}^{t}e_{th} + \delta_{ij}\dfrac{\nu}{(1-2\nu)}\Delta {}^{t}e_{kk} \right] \\ \quad + {}^{t}g_1 \displaystyle\sum_{n=1}^{N} D_n \left(\exp\left[-\lambda_n \Delta {}^{t}\Psi\right] - 1 \right) \left[{}^{t-\Delta t}q_{ij,n} + \frac{1}{3}\delta_{ij}\,{}^{t-\Delta t}q_{kk,n} \right] \end{array} \right) \tag{22}$$

where

$${}^{t}\overline{\mathrm{H}} = \sum_{n=1}^{N} D_n \left(1 - \frac{1-\exp\left[-\lambda_n \Delta {}^{t}\Psi\right]}{\lambda_n \Delta {}^{t}\Psi} \right) \tag{23}$$

5. The finite element model

The FEM as a numerical tool allows for solving such complex nonlinear viscoelastic problems undergoing large thermo-mechanical deformations with real boundary conditions. In the present formulation, the external load is taken to be deformation-dependent. The principle of virtual work, in the framework of the total Lagrange incremental formulation, can be stated as; Bathe (1996)

$$\int_{{}^{0}\mathrm{V}} {}_{0}^{t}S_{ij}\ {}_{0}^{t}\delta e_{ij}\ {}^{0}d\mathrm{V} - \int_{{}^{0}\mathrm{V}} {}_{0}^{t}f_i\ \delta u_i\ {}^{0}d\mathrm{V} - \int_{{}^{0}\Gamma_f} {}_{0}^{t}F_i\ \delta u_i\ {}^{0}d\Gamma = 0 \tag{24}$$

where δe_{ij} is the variation in the Green-strain vector caused by the virtual displacements δu_i. Since the stresses ${}_{0}^{t}S_{ij}$ and strains ${}_{0}^{t}e_{ij}$ are unknown, for solution; the following incremental decomposition is used;

$${}_{0}^{t}S_{ij} = {}_{0}^{t-\Delta t}S_{ij} + {}_{0}^{t}\Delta S_{ij} \quad \text{and} \quad {}_{0}^{t}e_{ij} = {}_{0}^{t-\Delta t}e_{ij} + {}_{0}^{t}\Delta e_{ij} \tag{25}$$

Eq. (22) can be rewritten as

$${}_{0}^{t}\Delta S_{ij} = {}_{0}^{t}C_{ijkl}^{nve}\ {}_{0}^{t}\Delta e_{kl} + {}^{t-\Delta t}{}_{0}\Delta S_{ij}^{h} - {}_{0}^{t}\Delta S_{ij}^{th} \tag{26}$$

where ${}_{0}^{t}C_{ijkl}^{nve}$ is the nonlinear viscoelastic stress-strain relation matrix, ${}^{t-\Delta t}{}_{0}\Delta S_{ij}^{h}$ is the stress increment which expresses the material history and ${}_{0}^{t}\Delta S_{ij}^{th}$ is the incremental thermal stress vector. Substitution of Eqs. (25)-(26) into Eq. (24) yields

$${}_{0}^{t}\left(\left[\mathrm{K}_L\right]+\left[\mathrm{K}_N\right]\right)\left\{\Delta\mathrm{u}\right\} = {}^{t}\left\{\mathrm{F}_{ext}\right\} + {}_{0}^{t}\left\{\mathrm{F}_{th}\right\} - {}_{0}^{t}\left\{\mathrm{F}_{int}\right\} \tag{27}$$

which represents a nonlinear equation for the incremental displacement vector $\{\Delta\mathrm{u}\}$. All matrix elements correspond to the configuration at time t and are defined with respect to the configuration at time 0. All terms in Eq. (27) will be completely defined in the following section.

6. The solution algorithm

This section presents the solution procedure of the developed FE model. It is important to realize that Eq. (27) contains two possible sources of nonlinearities; material nonlinearity due to nonlinear stress-strain relationships considering time-temperature-stress dependency of the material characteristics and geometric nonlinearity due to large displacements and rotations. Hence, linearization of Eq. (27) may introduce errors, which ultimately result into solution instability, and thus it cannot be solved by direct methods. For this reason, to obtain the solution at any time increment, the Newton-Raphson iterative scheme is used. Now, assuming that the equilibrium configuration at the time t-Δt is known and within the time t, it is postulated that (r) iterations have been performed. That is, given the stresses ${}^{t}\{\mathrm{S}\}^{(r)}$, ${}^{t}\{\mathrm{S}^{h}\}^{(r)}$, ${}^{t}\{\mathrm{S}^{th}\}^{(r)}$ and displacements ${}^{t}\{\mathrm{u}\}^{(r)}$ that satisfy the equilibrium equations. The solution algorithm to determine the equilibrium configuration at the time t can be described as follows.

1. Compute the linear and nonlinear counterparts of the overall stiffness matrix

$$ {}_0^t\left[\mathrm{K}_L\right]^{(r)} = \sum_{e=1}^{NE} \int_{{}^0\mathrm{V}^e} {}_0^t\left[\mathrm{B}_L\right]^{(r)T} {}_0^t\left[\mathrm{C}^{nve}\right]^{(r)} {}_0^t\left[\mathrm{B}_L\right]^{(r)} {}^0 d\mathrm{V}^e \tag{28a} $$

$$ {}_0^t\left[\mathrm{K}_N\right]^{(r)} = \sum_{e=1}^{NE} \int_{{}^0\mathrm{V}^e} {}_0^t\left[\mathrm{B}_N\right]^{(r)T} {}_0^t\left[\mathrm{S}\right]^{(r)} {}_0^t\left[\mathrm{B}_N\right]^{(r)} {}^0 d\mathrm{V}^e \tag{28b} $$

where *NE* is the total number of FEs. **[**B_L] and **[**B_N] are the linear and nonlinear strain-displacement transformation matrices, [S] is a matrix of 2nd Piola Kirchhoff stresses.

2. Compute the external force vector due to body forces and surface tractions and thermal force vector due to the incremental thermal strain, respectively

$$ {}^t\left\{\mathrm{F}_{ext}\right\}^{(r)} = \sum_{e=1}^{NE} \int_{{}^t\mathrm{V}^e} {}^t\left[\mathrm{N}^e\right]^{(r)} {}^t\left\{\mathrm{f}^e\right\}^{(r)} {}^t d\mathrm{V}^e + \sum_{e=1}^{NE} \int_{{}^t\Gamma^e} {}^t\left[\mathrm{N}^s\right]^{(r)} {}^t\left\{\mathrm{F}^e\right\} {}^t d\Gamma^e \tag{29} $$

$$ {}_0^t\left\{\mathrm{F}_{th}\right\}^{(r)} = \sum_{e=1}^{NE} \int_{{}^0\mathrm{V}^e} {}_0^t\left[\mathrm{B}_L\right]^{(r)T} {}_0^t\left\{\Delta\mathrm{S}^{th}\right\}^{(r)} {}^0 d\mathrm{V}^e \tag{30} $$

where [N^e] and [N^s] are the element and line shape function matrices, respectively.

3. Compute the internal force vector due to both the material damping and the internal stresses

$$ {}_0^t\left\{\mathrm{F}_{int}\right\}^{(r)} = \sum_{e=1}^{NE} \int_{{}^0\mathrm{V}^e} {}_0^t\left[\mathrm{B}_L\right]^{(r)T} {}_0^t\left\{\Delta\mathrm{S}^h + \hat{\mathrm{S}}\right\}^{(r)} {}^0 d\mathrm{V}^e \tag{31} $$

where {S^} a vector of 2nd Piola Kirchhoff stresses.

4. Compute the incremental displacement vector ${}^t\{\Delta\mathrm{u}\}^{(r+1)}$ by solving Eq. (27).

5. Update the displacement field

$$ {}^t\left\{\mathrm{u}\right\}^{(r+1)} = {}^t\left\{\mathrm{u}\right\}^{(r)} + \left\{\Delta\mathrm{u}\right\}^{(r+1)} \tag{32} $$

6. Compute and update the Green strain vector

$$ {}^t\left\{\Delta\mathrm{e}\right\}^{(r+1)} = {}_0^t\left[\mathrm{B}_L\right]^{(r+1)} {}^t\left\{\Delta\mathrm{u}\right\}^{(r+1)} \quad \text{and} \quad {}^t\left\{\mathrm{e}\right\}^{(r+1)} = {}^t\left\{\mathrm{e}\right\}^{(r)} + {}^t\left\{\Delta\mathrm{e}\right\}^{(r+1)} \tag{33} $$

7. Compute the nonlinear relaxation matrix using Eqs. (22) and (26), i.e., for plane stress analysis

$$ {}_0^t\left[\mathrm{C}^{nve}\right]^{(r+1)} = \frac{1}{\left({}_0^t g_0^{(r)} D_0 + {}_0^t\left[g_1\, {}_0^t g_2\, {}_0^t\bar{\mathrm{H}}\right]^{(r)}\right)(1-\nu^2)} \begin{bmatrix} 1 & \nu & 0 \\ \nu & 1 & 0 \\ 0 & 0 & 0.5(1-\nu) \end{bmatrix} \tag{34} $$

8. Compute the incremental thermal stress vector

$$ {}_0^t\left\{\Delta\mathrm{S}^{th}\right\}^{(r+1)} = {}_0^t\left[\mathrm{C}^{nve}\right]^{(r+1)} {}^t\left\{\Delta\mathrm{e}^{th}\right\} \tag{35} $$

9. Update the 2nd Piola Kirchhoff stress vector

$$ \begin{aligned} {}_0^t\left\{\Delta\mathrm{S}\right\}^{(r+1)} &= {}_0^t\left[\mathrm{C}^{nve}\right]^{(r+1)} {}^t\left\{\Delta\mathrm{e}\right\}^{(r+1)} + {}_0^t\left\{\Delta\mathrm{S}^h\right\}^{(r)} - {}_0^t\left\{\Delta\mathrm{S}^{th}\right\}^{(r+1)} \\ {}_0^t\left\{\mathrm{S}\right\}^{(r+1)} &= {}_0^t\left\{\mathrm{S}\right\}^{(r)} + {}_0^t\left\{\Delta\mathrm{S}\right\}^{(r+1)} \end{aligned} \tag{36} $$

10. Compute the equivalent Von Mises stress

$$ {}_0^t S_e^{(r+1)} = \sqrt{\frac{3}{2}\, {}_0^t\{\mathrm{S}\}^{(r+1)}\, {}_0^t\{\mathrm{S}\}^{(r+1)}} \tag{37} $$

11. Update the nonlinear stress and temperature parameters.
12. Compute the incremental and updating the reduced time

$$ {}_0^t\Delta\Psi^{(r+1)} = \frac{\Delta t}{{}_0^t a^{(r+1)}} \quad \text{and} \quad {}_0^t\Psi^{(r+1)} = \frac{t}{{}_0^t a^{(r+1)}} \tag{38} $$

13. Compute the quantity defined by Eq. (23)

$$ {}_0^t\overline{\mathrm{H}}^{(r+1)} = \sum_{n=1}^{N} D_n \left(\frac{\lambda_n\, {}_0^t\Delta\Psi^{(r+1)} + \exp\left[-\lambda_n\, {}_0^t\Delta\Psi^{(r+1)}\right] - 1}{\lambda_n\, {}_0^t\Delta\Psi^{(r+1)}} \right) \tag{39} $$

14. Compute the incremental stress vector due to material history, using Eqs. (22) and (26); i.e., for plane stress analysis

$$ \begin{gathered} {}_0^t\left\{\Delta\mathrm{S}^h\right\}^{(r+1)} = \frac{{}_0^t g_1^{(r+1)}\, \overline{\mathrm{E}}^{(r+1)}}{3\left({}_0^t g_0^{(r+1)} D_0 + {}_0^t\left[g_1\; g_2\; \overline{\mathrm{H}}\right]^{(r+1)}\right)(1-\nu)} \begin{bmatrix} 4-5\nu & 1-2\nu & 0 \\ 1-2\nu & 4-5\nu & 0 \\ 0 & 0 & 3(1-\nu) \end{bmatrix}, \\ \overline{\mathrm{E}}^{(r+1)} = \sum_{n=1}^{N} D_n \left(\exp\left[-\lambda_n\, {}_0^t\Delta\Psi^{(r+1)}\right] - 1 \right) {}_0^t\{\mathrm{q}_n\}^{(r)} \end{gathered} \tag{40} $$

15. Compute the material history vector using Eq. (17)

$$ {}_0^t\{\mathrm{q}_n\}^{(r+1)} = \exp\left(-\lambda_n\, {}_0^t\Delta\Psi^{(r+1)}\right) {}_0^t\{\mathrm{q}_n\}^{(r)} + \frac{1-\exp\left(-\lambda_n\, {}_0^t\Delta\Psi^{(r+1)}\right)}{\lambda_n\, {}_0^t\Delta\Psi^{(r+1)}}\, {}_0^t\left[\left(g_2\{\mathrm{S}\}\right)^{(r+1)} - \left(g_2\{\mathrm{S}\}\right)^{(r)}\right] \tag{41} $$

16. Steps 1 to 15 are repeated till the displacement convergence is satisfied

$$ \left\|\{\Delta\mathrm{u}\}^{(r+1)}\right\| \Big/ \left\| {}^t\{\mathrm{u}\}^{(r+1)} \right\| < Tol, \quad Tol \text{ is a very small value.} \tag{42} $$

17. Once the convergence is satisfied, update the state at the end of the time increment

$$ {}^t\{\mathrm{u}\} \leftarrow {}^t\{\mathrm{u}\}^{(r+1)}, \quad {}_0^t\{\mathrm{S}\} \leftarrow {}_0^t\{\mathrm{S}\}^{(r+1)}, \text{ and } \quad {}_0^t\{\mathrm{q}_n\} \leftarrow {}_0^t\{\mathrm{q}_n\}^{(r+1)} \tag{43} $$

18. Solution proceeds to the next time step for which steps 1 through 17 are repeated.

7. Applications

The applicability of the developed model to predict the response of nonlinear viscoelastic structures undergoing large deformations is investigated. Two problems with different thermal/mechanical loading conditions will be analyzed.

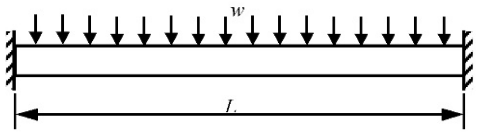

Fig. 1 A viscoelastic beam under uniform distributed load

Table 1 Coefficients of the Prony series

n	$D_n\times10^{-5}$ (MPa^{-1})	λ_n (s^{-1})
1	2.36358	1.0
2	0.566016	10^{-1}
3	1.48405	10^{-2}
4	1.88848	10^{-3}
5	2.85848	10^{-4}
6	4.00569	10^{-5}
7	6.04235	10^{-6}
8	7.96477	10^{-7}
9	16.2179	10^{-8}
D_o=27.09x10^{-5} MPa^{-1}		

7.1 Thermo-mechanical response of a beam

Consider a viscoelastic beam of length L=2540 mm and cross section 25.4 mm×25.4 mm as shown in Fig. 1, with material properties given in Table 1. For nonlinear viscoelastic behavior (NLVE), fourth-order polynomials are sufficient for calibrating the nonlinear stress-dependent functions, Haj-Ali and Mulina (2004)

$$ {}^{t}_{0}g^{k}_{\sigma j} = 1+\sum_{i=1}^{n\sigma j}\kappa^{i}_{\sigma j}\left\langle\frac{{}^{t}_{0}S^{k}_{e}-\sigma_{\mathrm{o}}}{\sigma_{\mathrm{o}}}\right\rangle^{i}, \qquad {}^{t}_{0}a^{k}_{\sigma} = 1+\sum_{i=1}^{n\sigma}\delta^{i}_{\sigma}\left\langle\frac{{}^{t}_{0}S^{k}_{e}-\sigma_{\mathrm{o}}}{\sigma_{\mathrm{o}}}\right\rangle^{i} \qquad j=0,1,2 \qquad (44) $$

where $<x>=0$ for $x\le 0$ and $<x>=x$ for $x>0$.

The parameters describing these functions are given in Table 2. The Poisson's ratio v of the material, which is assumed to be time-invariant, is taken 0.4, Payette and Reddy (2010), and the effective stress σ_{o} is taken 2.75 MPa. The problem is analyzed with plane stress condition. At t =0 the beam is subjected to a time invariant uniform vertical distributed load w=0.0437817 N/mm. The load at t =0 s is applied incrementally to insure convergence of the solution. Table 3 presents some selected numerical results for the maximum vertical deflection of linear viscoelastic (LVE) and NLVE beam under uniform distributed load. It is noted that, the obtained numerical results for LVE analysis are in an excellent agreement with those of Payette and Reddy (2010).

Furthermore, the maximum deflection for corresponding linear and nonlinear elastic solutions, where the Young's modulus is 3691.45 MPa, is obtained as 22.1246 and 23.22611 mm, respectively. Thus at t=0 s, the obtained results for LVE and NLVE coincide with the corresponding elastic solutions. In addition, it is noticeable that the deflection for NLVE is greater than that for LVE. This is owing to the effect of the nonlinear stress parameters on increasing the compliance of the beam. Fig. 2 illustrates the relaxation of the maximum equivalent Von Mises stress with time.

Table 2 Nonlinear stress dependent parameters in the Schapery model

	κ^1_σ	κ^2_σ	κ^3_σ	κ^4_σ
g_0	0.183	0.567	-1.067	0.533
g_1	0.067	0.133	2.133	-2.133
g_2	-0.773	9.707	-5.787	8.533
a_σ	δ^1_σ	δ^2_σ	δ^3_σ	δ^4_σ
	-0.373	2.580	-5.227	3.520

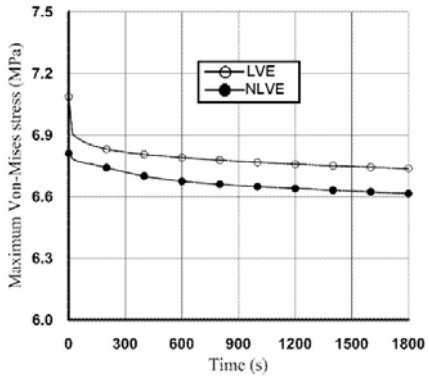

Fig. 2 Maximum Von Mises stress of LVE and NLVE beam behaviors

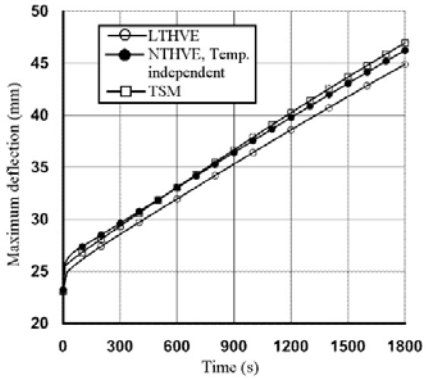

Fig. 3 Maximum deflection for different Thermo-viscoelastic beam behaviors

To investigate the effect of thermal load upon the beam response, the beam will be subjected to a thermal load represented by a prescribed temperature ${}^t\theta$=303+0.00833t K, in addition to the time invariant uniform vertical distributed load. Numerical results for different thermo-rheological behaviors are obtained; namely LTHVE, NLTHVE in which the material nonlinearity is attributed to the nonlinear stress-dependent parameters only, and TSM. For TSM, the time temperature shift factor is approximated as, Lai and Bakker (1996)

$$a_\theta(t) = \exp\left(\frac{-17({}^t\theta - \theta_{ref})}{56 + ({}^t\theta - \theta_{ref})}\right) \tag{45}$$

Fig. 3 displays the maximum thermo-mechanical vertical deflection of the beam for LTHVE, NLTHVE, and TSM behaviors. Also, the maximum equivalent Von Mises stress is illustrated in Fig. 4. It is depicted that the thermo-rheological behavior has a great significant effect on the Von Mises stress, especially as the time marches. This is due to that the nonlinear stress parameters and the time-temperature shift factor result in decreasing the beam stiffness and hence lower equivalent Von Mises stresses is obtained.

An important characteristic of the viscoelastic constitutive model employed in this work is that the body should eventually return to its original configuration once the loads are removed. To demonstrate that the developed FE model capture this effect, the beam will be subjected to the following quasi-static transverse load

$$w(t) = w_0\left\{H(t) - \frac{1}{\tau(\gamma-\mu)}\left[(t-\mu\tau)H(t-\mu\tau) - (t-\gamma\tau)H(t-\gamma\tau)\right]\right\} \tag{46}$$

Table 3 FE results for the maximum deflection (mm)

Time, (s)	LVE (Payette and Reddy (2010))	LVE (Present)	NLVE (Present)
0	23.13940	23.12460	23.22611
200	25.40000	25.36917	25.84787
400	25.62606	25.60196	26.06863
600	25.76576	25.74364	26.22378
800	25.87498	25.85673	26.34709
1000	25.96642	25.95250	26.45129
1200	26.04770	26.03488	26.54081
1400	26.11628	26.10641	26.61843
1600	26.17724	26.16902	26.68629
1800	26.23058	26.22430	26.74613

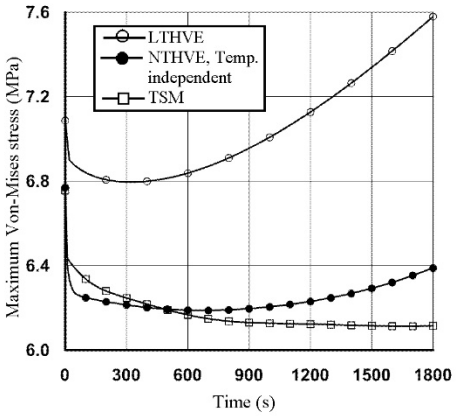

Fig. 4 Maximum Von Mises stress for different thermo-viscoelastic beam behaviors

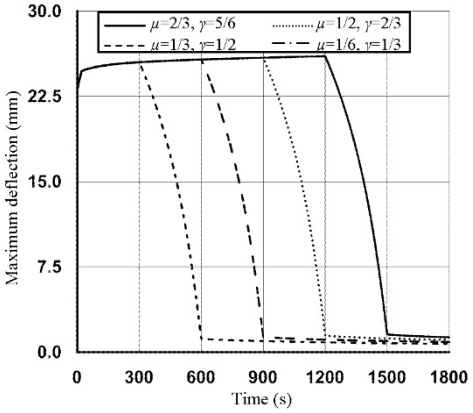

Fig. 5 Maximum deflection of NLVE beam subjected to time-dependent transverse loading

where w_0=0.0437817 N/mm and τ=1800 s. The parameters $0\leq\mu\leq\gamma\leq1$ are constants. Fig. 5 presents the results for NLVE analysis with σ_o=2.75 MPa at different values of μ and γ. It is evident that the beam recovers its original configuration as t tends to infinity once the applied load is removed.

7.2 Thermo-mechanical response of a composite cylinder

Consider a thick viscoelastic cylinder covered by a perfectly bonded aluminum layer as shown in Fig. 6. Plane strain condition is assumed. The layer is assumed to behave linear elasticity, while the viscoelastic cylinder is simulated using six terms of the Prony exponential series, Touati and Cederbaum (1998b). The elastic and thermal properties of the viscoelastic cylinder as well as the Prony series coefficients are given in Table 4. The nonlinear material functions based on stress and temperature are given by the following functions

$$g_0^\sigma(t)=1+0.15\tilde{\mathrm{S}},\ g_1^\sigma(t)=1+1.435\tilde{\mathrm{S}}^{2.4},\ g_2^\sigma(t)=1+0.75\tilde{\mathrm{S}}^2,\ a^\sigma(t)=\exp\left(-1.75\tilde{\mathrm{S}}\right),\ \tilde{\mathrm{S}}=\frac{{}^tS_e}{\sigma_o} \quad (47)$$

$$g_0^\theta(t)=1+0.91\tilde{\theta},\ g_1^\theta(t)=\exp\left(-8.5\tilde{\theta}\right),\ g_2^\theta(t)=\exp\left(-12.12\tilde{\theta}\right),\ a^\theta(t)=\exp\left(-40\tilde{\theta}\right),\ \tilde{\theta}=\frac{{}^t\theta-\theta_{ref}}{\theta_{ref}} \quad (48)$$

Table 4 Thermal and elastic properties and coefficients of the Prony series

n	D_nx10^{-4} (MPa^{-1})	λ_n (s^{-1})
1	0.210	1.0
2	0.216	10^{-1}
3	0.118	10^{-2}
4	0.159	10^{-3}
5	0.216	10^{-4}
6	0.201	10^{-5}
D_o=3.69004x10^{-4} MPa^{-1} v=0.35, α=5x10^{-5} ^{o}C^{-1} σ_o=100 MPa , θ_{ref}=303 K		

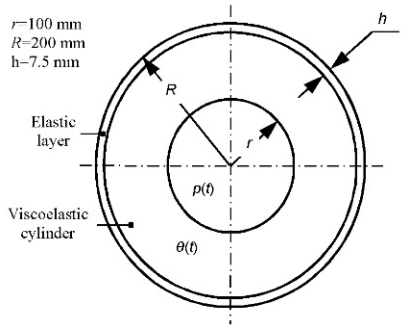

Fig. 6 A composite thick cylinder subjected to a quasi-static thermo-mechanical load

where σ_o is the effective stress limit and θ_{ref} is the reference temperature of the material. The thermal and elastic properties of the aluminum layer are: E=70 GPa, v=0.33, and α=7.17x10^{-6} ^{o}C^{-1}.

The cylinder is subjected to a quasi-static thermo-mechanical loading; a prescribed space-wise ramp temperature $\theta(t)$ as a thermal load and an internal pressure $p(t)$ as a mechanical load. The space-wise ramp temperature is $\theta(t)$=303+0.9t K, while the acting internal pressure has the following quasi-static loading-unloading pattern

$$p(t)=\begin{cases} p_0\left(t/\mu\tau\right), & \text{for } \ 0\le t\le \mu\tau \\ p_0\left(t-\gamma\tau\right)/\left[\left(\mu-\gamma\right)\tau\right], & \text{for } \ \mu\tau\le t\le \gamma\tau \end{cases} \tag{49}$$

where p_0=100 MPa, μ=0.5, γ=1.0, and τ =100 s.

The inner radial displacement is shown in Figs. 7(a) and (b) for viscoelastic and thermo-viscoelastic analyses, respectively. It is noticed that the modeling the cylinder as nonlinear viscoelastic has a notable significant effect on the creep rate of the radial displacement. Also, for LVE and NLVE analyses, it is depicted that the cylinder recovers its original configuration as t tends to infinity once the applied load is removed.

Figs. 8(a) and (b) illustrate the variation of the maximum equivalent Von Mises stress on the inner surface with time for viscoelastic and thermo-viscoelastic analysis, respectively. It is depicted that the nonlinear stress functions greatly influence the stress. In addition, it is found that the thermo-rheological behavior has a dramatic effect on the system response. This is owing to the effect of the nonlinear-temperature parameters and time-temperature shift factor on the creep compliance of the cylinder.

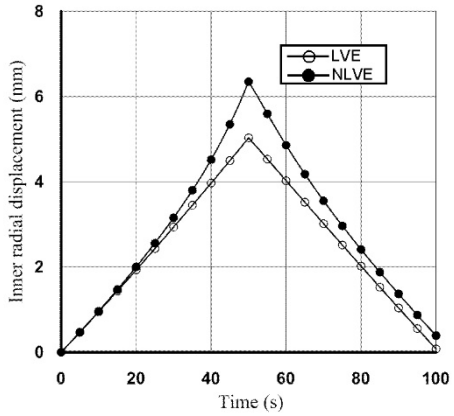

Fig. 7(a) Creep of the inner radial displacement for viscoelastic analysis

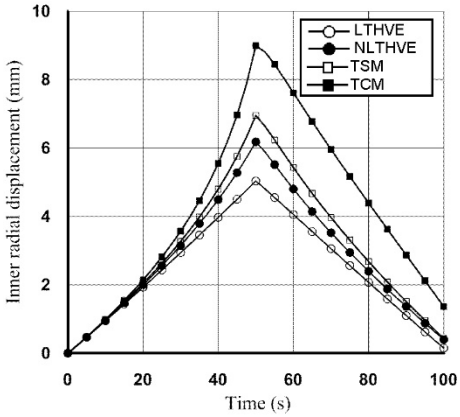

Fig. 7(b) Creep of the inner radial displacement for thermo-viscoelastic analysis

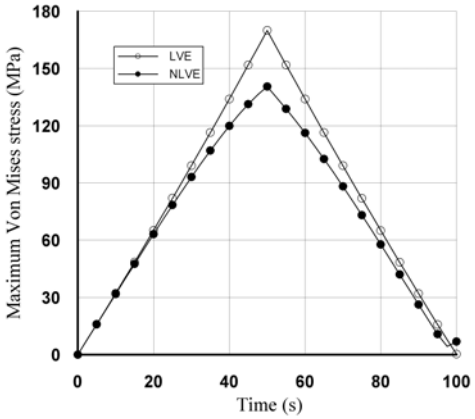

Fig. 8(a) Maximum Von Mises stress for viscoelastic analysis

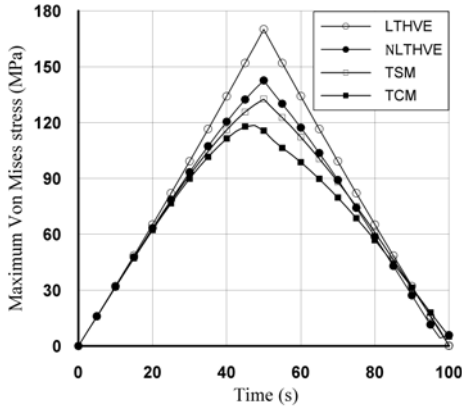

Fig. 8(b) Maximum Von Mises stress for thermo-viscoelastic analysis

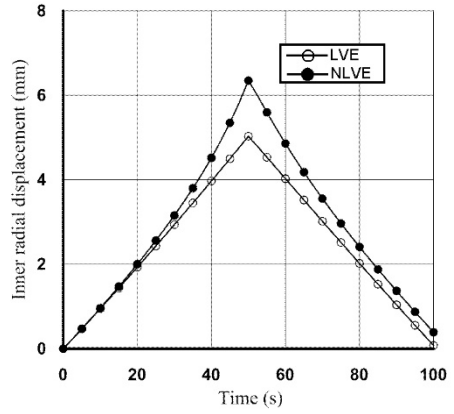

Fig. 9(a) Variation of the radial displacement with radius LVE analysis

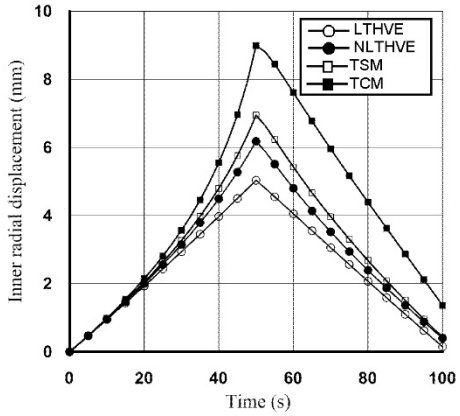

Fig. 9(b) Variation of the radial displacement with radius NLVE analysis

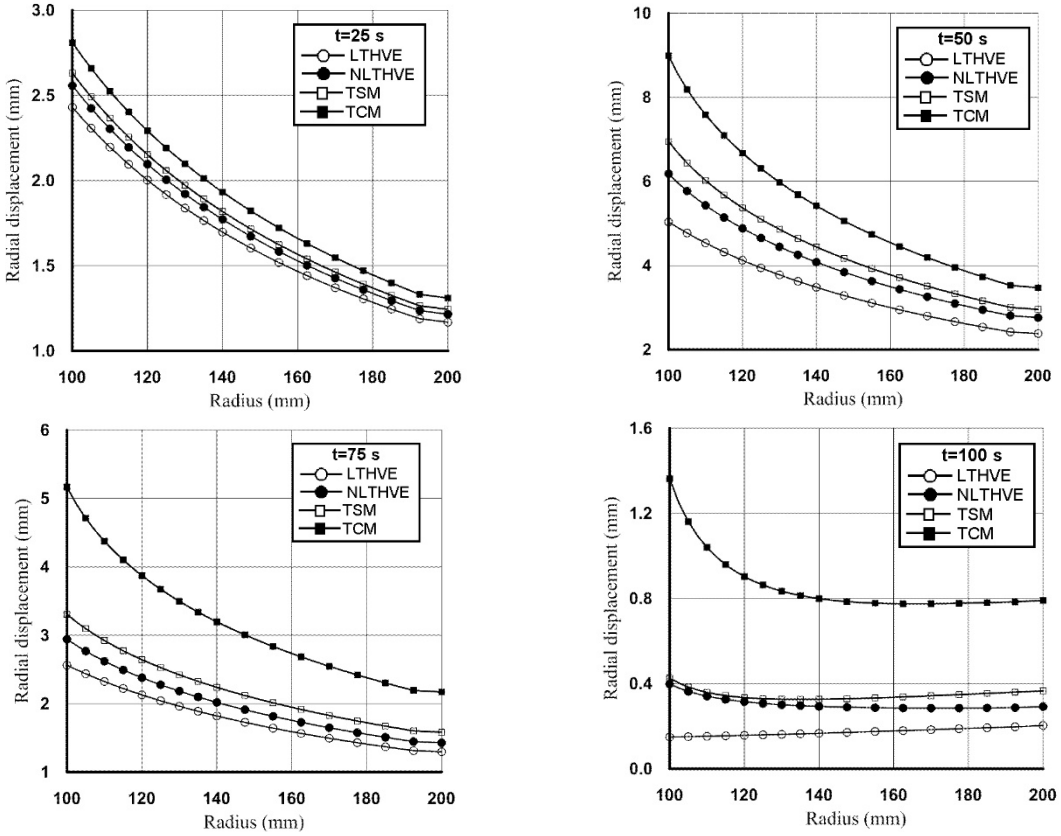

Fig. 10 Variation of the radial displacement with radius for thermo-viscoelastic analysis at various time

Table 5 Radial displacement of the inner surface for LVE and LTHVE analyses

	Time (s)					
	10	30	50	70	90	100
LVE	0.9469	2.9366	5.0289	3.0152	1.0378	0.0746
LTHVE	0.9471	2.9388	5.0340	3.0571	1.1021	0.1495

Figs. 9 and 10 show the variation of the radial displacement with radius for viscoelastic and thermo-viscoelastic analyses, respectively.

The effect of the effective stress limit σ_o on the system response will be studied. Table 5 provides some numerical results for the inner radial displacement for LVE and LTHVE analyses (σ_o is taken infinity and all nonlinear temperature parameters are assumed to equal unity). Tables 6-8 present the inner radial displacement while varying the effective stress limit for different loading conditions and thermo-rheological behaviors. From the obtained results, it can be clear that when the effective stress limit increases, the radial displacement decreases. Also, the effect of the effective stress limit is more significant while the time marches. The effect on TCM behavior is more than that on the TSM and NLVE behaviors; this is attributed to the complex effect of the nonlinear-temperature parameters. For example at t=50 s and for TCM behavior, the radial displacement decreases with 23.84% as the effective stress limit increased from 100 to 180 MPa.

Table 6 The variation of inner radial displacement for different effective stress limits (NLVE behavior)

Time (s)	Effective stress limit σ_o (MPa)				
	100	120	140	160	180
10	0.9612	0.9497	0.9480	0.9467	0.9457
30	3.1545	3.0717	3.0391	3.0175	3.0023
50	6.3479	5.7615	5.5570	5.4328	5.3510
70	3.5515	3.3103	3.2259	3.1743	3.1401
90	1.3681	1.1903	1.1378	1.1071	1.0878
100	0.3873	0.21674	0.1668	0.1380	0.1198

Table 7 The variation of inner radial displacement for different effective stress limits (TSM behavior)

Time (s)	Effective stress limit σ_o (MPa)				
	100	120	140	160	180
10	0.9720	0.9693	0.9674	0.9661	0.9650
30	3.2684	3.2027	3.1633	3.1375	3.1194
50	6.9483	6.3862	6.0861	5.9045	5.7853
70	3.9674	3.7197	3.5833	3.4996	3.4443
90	1.5114	1.3530	1.269	1.2194	1.1879
100	0.4266	0.2737	0.1929	0.1453	0.1151

Table 8 The variation of inner radial displacement for different effective stress limits (TCM behavior)

Time (s)	Effective stress limit σ_o (MPa)				
	100	120	140	160	180
10	0.9897	0.9867	0.9847	0.9832	0.9822
30	3.5674	3.4789	3.4264	3.3923	3.3687
50	8.9904	7.8982	7.3615	7.0482	6.8467
70	5.9589	5.1961	4.8146	4.5911	4.4475
90	2.8712	2.2816	1.9901	1.8220	1.7160
100	1.3634	0.8005	0.5218	0.3613	0.2603

Whereas, for the same conditions, the radial displacement decreases with 15.7% and 16.74% for NLVE and TSM behaviors, respectively.

8. Conclusions

An efficient and accurate computational FE model for investigating the nonlinear viscoelastic response of thermo-rheological complex structures under different thermal/mechanical loading histories is developed. The model is derived based on implicit stress integration solutions for large displacements and rotations (with small strains) and quasistatic thermo-mechanical problems. The Schapery's single-integral creep nonlinear viscoelastic model is modified for a time-stress-temperature-dependent behavior. An incremental-recursive relationship for the constitutive equations is derived, such that history data need only be stored from the previous time step. Both material and geometrical nonlinearities are modeled in the framework of the total Lagrangian description. The Newton-Raphson iterative scheme is used for solving the resulting nonlinear incremental equilibrium equations. The developed model is verified by comparing the obtained

results with benchmark results and an excellent agreement is found. Two different examples are analyzed to demonstrate the applicability of the developed model. The obtained results show that, the effective stress limit (level of material nonlinearity) and thermo-rheological behavior have notable significant effects on the system response. Therefore, dependency of viscoelastic material parameters on the stress and/or temperature should be modelled carefully.

References

Areias, P. and Matouš, K. (2008), "Finite element formulation for modeling nonlinear viscoelastic elastomers", *Comput. Meth. Appl. Mech. Eng.*, **197**(51), 4702-4717.

Bathe, K.J. (1996), *Finite Element Procedures*, Prentice–Hall Inc., Upper Saddle River, New Jersey, USA.

Bonet, J. (2001), "Large strain viscoelastic constitutive models", *Int. J. Solids and Struct.*, **38**(17), 2953-2968.

Christensen, R. (1982), *Theory of Viscoelasticity: An Introduction*, Access Online via Elsevier.

Feng, W.W. (1992), "A recurrence formula for viscoelastic constitutive equations", *Int. J. Non Linear Mech*., **27**(4), 675-678.

Ferry, J.D. (1980), *Viscoelastic Properties of Polymers*, Wiley, New York.

Fung, Y.Y.C. and Tong, P. (2001), *Classical and Computational Solid Mechanics*, World Scientific.

Guedes, R.M. (2010), "Nonlinear viscoelastic analysis of thick-walled cylindrical composite pipes", *Int. J. of Mech. Sci.*, **52**(8), 1064-1073.

Haj-Ali, R.M. and Muliana, A.H. (2004), "Numerical finite element formulation of the Schapery non-linear viscoelastic material model", *Int. J. Numer. Meth. Eng.*, **59**(1), 25-45.

Harper, B. and Weitsman, Y. (1985), "Characterization method for a class of thermorheologically complex materials", *J. Rheol.*, **29**, 49-66.

Holzapfel, G. and Reiter, G. (1995), "Fully coupled thermomechanical behaviour of viscoelastic solids treated with finite elements", *Int. J. Eng. Sci.*, **33**(7), 1037-1058.

Johnson, A.R. and Chen, T.K. (2005), "Approximating thermo-viscoelastic heating of largely strained solid rubber components", *Comput. Meth. Appl. Mech. Eng.*, **194**(2), 313-325.

Khan, A.S., Baig, M., Hamid, S. and Zhang, H. (2010), "Thermo-mechanical large deformation responses of Hydrogenated Nitrile Butadiene Rubber (HNBR): experimental results", *Int. J. Solids and Struct*., **47**(20), 2653-2659.

Khan, A.S., Lopez-Pamies, O. and Kazmi, R. (2006), "Thermo-mechanical large deformation response and constitutive modeling of viscoelastic polymers over a wide range of strain rates and temperatures", *Int. J. Plast.*, **22**(4), 581-601.

Lai, J. and Bakker, A. (1996), "3-D Schapery representation for non-linear viscoelasticity and finite element implementation", *Comput. Mech.*, **18**(3), 182-191.

Mahmoud, F.F., El-Shafei, A.G. and Attia, M.A. (2011), "Analysis of thermoviscoelastic frictionless contact of layered bodies", *Finite Elem. Anal. Des.*, **47**(3), 307-318.

Muliana, A.H. (2008), "Multi-scale framework for the thermo-viscoelastic analyses of polymer composites", *Mech. Res. Commun.*, **35**(1), 89-95.

Payette, G. and Reddy, J. (2010), "Nonlinear quasi-static finite element formulations for viscoelastic Euler–Bernoulli and Timoshenko beams", *Int. J. Numer. Meth. Biomed. Eng.*, **26**(12), 1736-1755.

Peretz, D. and Weitsman, Y. (1983), "The nonlinear thermoviscoelastic characterizations of FM-73 adhesives", *J. Rheol.*, **27**, 97-114.

Reese, S. and Govindjee, S. (1997), "Theoretical and numerical aspects in the thermo-viscoelastic material behaviour of rubber-like polymers", *Mech. of Time-Depend. Mater*., **1**(4), 357-396.

Reese, S. and Wriggers, P. (1998), "Thermoviscoelastic material behaviour at finite deformations with temperature–dependent material parameters", *ZAMM Appl. Math. Mech.*, **78**, S157.

Rogers, T.G. and Lee, E.H. (1992) "On the Finite Deflection of a Viscoelastic Cantilever", *Proceedings of*

4th U.S. Nat1 Cong. of Appl. Mech., ASME, 977-987.
Roy, S. and Reddy, J. (1988), "Finite-element models of viscoelasticity and diffusion in adhesively bonded joints", *Int. J. Numer. Meth. Eng.*, **26**(11), 2531-2546.
Schapery, R.A. (1969), "On the characterization of nonlinear viscoelastic materials", *Polym. Eng. Sci.*, **9**(4), 295-310.
Schapery, R.A. (1997), "Nonlinear viscoelastic and viscoplastic constitutive equations based on thermodynamics", *Mech. Time-Depend. Mater.*, **1**(2), 209-240.
Taylor, R.L., Pister, K.S. and Goudreau, G.L. (1970), "Thermomechanical analysis of viscoelastic solids", *Int. J. Numer. Method. Eng.*, **2**(1), 45-59.
Touati, D. and Cederbaum, G. (1998a), "Postbuckling of non-linear viscoelastic imperfect laminated plates. Part II: structural analysis", *Compos. Struct.*, **42** (1), 43-51.
Touati, D. and Cederbaum, G. (1998b), "Stress relaxation of nonlinear thermoviscoelastic materials predicted from known creep", *Mech. Time-Depend. Mater.*, **1**(3), 321-330.
Vaz, M.A. and Caire, M. (2010), "On the large deflections of linear viscoelastic beams", *Int. J. Non Linear Mech.*, **45**, 75-81.